New PCT probes featuring N-phenylmonoaza-18-crown-6 and aryl/pyridyl oxadiazoles: Optical spectral studies of solvent effects and selected metal ions

ARTICLE *in* JOURNAL OF INCLUSION PHENOMENA · OCTOBER 2008

Impact Factor: 1.49 · DOI: 10.1007/s10847-008-9441-5

5 AUTHORS, INCLUDING:

Tabrez Khan
The Scripps Research Institute
16 PUBLICATIONS **127** CITATIONS

J Incl Phenom Macrocycl Chem (2008) 62:81–90
DOI 10.1007/s10847-008-9441-5

ORIGINAL ARTICLE

New PCT probes featuring *N*-phenylmonoaza-18-crown-6 and aryl/pyridyl oxadiazoles: optical spectral studies of solvent effects and selected metal ions

Sabir H. Mashraqui · Subramanian Sundaram · Tabrez Khan · Shailesh Ghadigaonkar · Kirandevi Poonia

Received: 27 February 2008 / Accepted: 2 April 2008 / Published online: 23 April 2008

Abstract Aryl/pyridyl oxadiazole chromophores **6**, **8** and **10**, carrying *N*-phenyl aza-18-crown-6 have been synthesized as new photo-induced charge transfer (PCT) probes. While, the absorption spectra of the hosts experienced a slight negative solvatochromism, however the emission bands were dramatically red shifted (Stokes shifts up to 178 nm) in solvents of increasing polarity. Among the metal ions tested, Li^+, Na^+, K^+ and Mg^{2+} did not appreciably perturbed the optical properties of the hosts. On the other hand, Ba^{2+} and to a lesser extent Ca^{2+} induced marked blue shifts in both the absorption and emission spectra of the hosts. The magnitude of cation induced spectral blue shifts corresponded with the increasing acceptor strength of the attached aryl/pyridyl groups in the host molecules. The blue shifts and the stability constants were found to follow the order $Ba^{2+} > Ca^{2+} \gg Mg^{2+} > Na^+ > Li^+ > K^+$. Competitive experiments performed with a matrix of ions also revealed superior binding affinity of Ba^{2+} with all the hosts examined. Noteworthily, the deep yellow solution (λ_{max}, 386 nm) of the host **10** was completely bleached (λ_{max}, 320 nm), in the company of Ba^{2+} thereby allowing the naked eye detection of this ion.

Keywords *N*-Phenylmonoaza-18-crown-6-aryl/pyridyl oxadiazoles · Synthesis · Optical spectral studies · Solvatochromism · Metal ion interaction · Ba^{2+} selective optical probe

S. H. Mashraqui (✉) · S. Sundaram · T. Khan · S. Ghadigaonkar · K. Poonia
Department of Chemistry, University of Mumbai, Vidyanagari, Santacruz(E) 400098, India
e-mail: sh_mashraqui@yahoo.com

Introduction

The development of molecular probes capable of targeting metal ions selectively is a subject of current interest in supramolecular chemsitry because of implications in cell biology, medicine, analytical and environmental sciences [1]. Due to high sensitivity, ultra-fast response and real-time measurements, the optical spectral techniques are gaining increasing attention for the selective analysis of metal ions. While crown ethers show high affinities for alkali metal ions [2], in contrast aza-crown ethers exhibit superior interactions towards alkaline earth metal ion [3]. Furthermore, aza-15-crown-5 binds Mg^{2+} and Ca^{2+} selectively [4], but aza-18-crown-6, possessing an expanded cavity interacts relatively strongly with the larger Ba ions [3]. During the last decade, a variety of supramolecular motifs working on the principle of either photo-induced electron transfer [5] or photo-induced charge transfer (PCT) [6] probes have been designed for metal ion recognition. Though, a large number of Ca^{2+} and Mg^{2+} optical sensors have been described [7], surprisingly only a few chromogenic probes are known for Ba^{2+} [3]. Barium compounds find extensive uses in metallurgy and medical diagnostics [8]. However, many Barium salts are also environmental pollutants and toxic. Exposure to high concentrations, particularly in the work places and mining areas are reported to cause severe health problems [9]. Consequently, the development of colorimetric and fluorimetric sensors capable of selectively targeting Ba^{2+} is therefore of relevance in clinical medicine and environmental applications.

In connection with our ongoing research on metal ion sensors [10], we now wish to report synthesis and optical spectral studies of chromoionophores **6**, **8** and **10** featuring a common *N*-phenylmonoaza-18-crown-6 ring and aryl/pyridyl-oxadiazole motifs of differing acceptor strengths.

Monoaza-18-crown-6 was specifically chosen as a receptor for its binding preference for Ba^{2+} relative to alkali and other alkaline-earth metal ions. Chromoionophores **6**, **8** and **10** are designed to function as the PCT systems because of the direct conjugation between the donor *N*-phenyl aza-crown ether and the acceptors aryl/pyridyl-oxadiazole components. Furthermore, since acceptor strength increases in the order, 4-nitrophenyl > 4-pyridyl > *t*-butylphenyl, the charge transfer character is expected to follow the order **10** > **8** > **6**. In analogy to the known aza-crown based donor acceptor systems [3, 10d], the complexation of metal ion by the aza-crown receptor in **6**, **8** and **10** would result in the delinking of the nitrogen 'lone pair' from conjugation [10d] and diminish the charge transfer interaction existing in free hosts. Consequently, metal ion complexation is expected to induce blue shifts of the charge transfer bands associated with **6**, **8** and **10**.

The synthetic route implemented for **6**, **8** and **10** is depicted in Scheme 1. Condensation of the known *N*-phenylaza-18-crown-6 carboxaldehyde **1** [11] with the known 4-(*t*-butylphenyl)hydrazide (**2**) [12], Isoniazide (**3**) and 4-nitrophenylhydrazide (**4**) [13] gave the corresponding hydrazones **5**, **7** and **9**, respectively, in good yield. Oxidative cyclization of **5**, **7** and **9** using $KMnO_4$ in dry acetone [14] provided the target probes **6**, **8** and **10** in reasonable yields after SiO_2 column chromatographic purification of crude products. The structures of **6**, **8** and **10** were fully substantiated on the basis of elemental analysis and spectral data, which is summarized in the experimental section.

Experimental

Metal perchlorates were prepared as described in the literature [15] and dried under vacuum prior to use. The chemicals and spectral grade solvents were purchased from S.D. Fine Chemicals (India) and used as received. IR spectra were recorded on a Shimadzu FTIR-420 spectrophotometer. ^{1}H NMR spectra were recorded in $CDCl_3$ solution on a Bruker 300 MHz spectrometer with TMS as an internal standard. Coupling constants *J* are given in hertz. Elemental analyses were done on Carlo Erba instrument EA-1108 Elemental analyzer. UV–Vis spectra were recorded on Jasco V-530 UV–Vis spectrophotometer, fluorescence spectra were recorded on Hitachi F-4500 Fluorescence spectrophotometer.

Preparation of hydrazones **5**, **7** and **9**: general procedure

N-Phenylaza-18-crown-6 carboxaldehyde **1** and appropriate acid hydrazide (4 mmol, each) were dissolved in absolute ethanol (20 mL) and the reaction refluxed on a water-bath for about 3 h. The reaction mixture was then cooled to room temperature and the precipitated solid filtered, washed with cold ethanol and air dried to give the corresponding hydrazones.

*Preparation of hydrazone **5***

Following the general procedure, the condensation of **1** with 4-*t*-butylbenzoic hydrazide **2** afforded **5** as a pale yellow solid in 75% yield (1.426 g), mp, 122–124 °C.

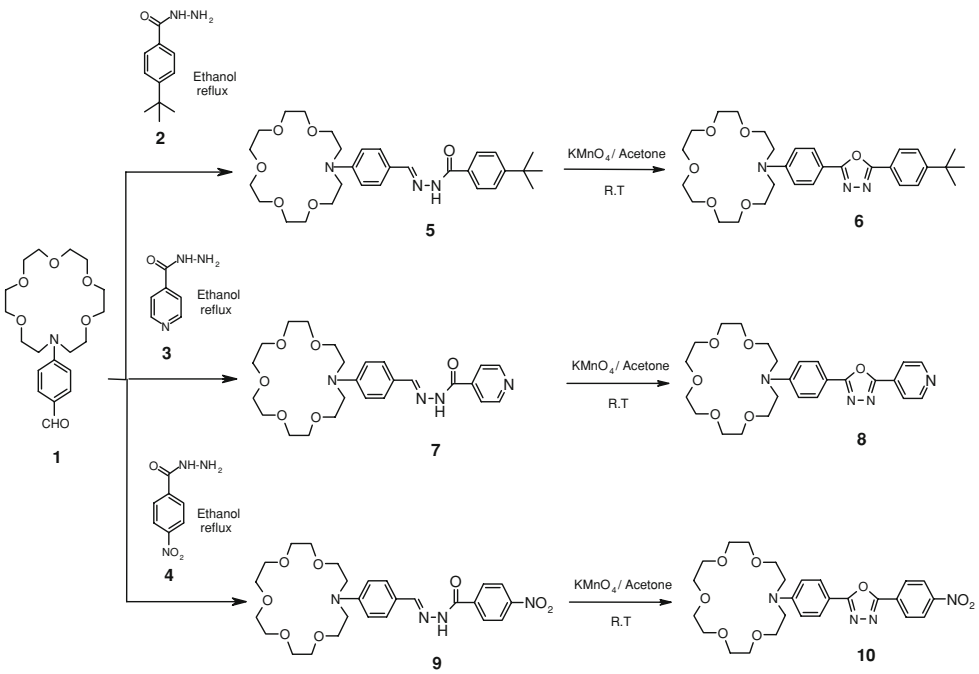

Scheme1 Aryl/pyridyl oxadiazole chromophores **6**, **8** and **10**

IR (KBr): 3198, 3039, 2954, 2866, 1637, 1609, 1594, 1521, 1359, 1303, 1284, 1183, 1123, 1064, 921, 854, 818, 767, 730 cm^{-1}. 1H-NMR (60 MHz, $CDCl_3$): δ, 9.82 (s, 1H, –NH–), 8.25 (s, 1H, –CH=N–), 7.78 (d, 2H, $J = 7$ Hz, Ar–H), 7.61 (d, 2H, $J = 8.5$ Hz, Ar–H), 7.45 (d, 2H, $J = 7$ Hz, Ar–H), 6.64 (d, 2H, $J = 8.5$ Hz, Ar–H), 3.80–3.31 (m, 24H, > NCH_2CH_2O–), 1.33 (s, 9H, Ar–$C(CH_3)_3$). Anal. Calcd for $C_{30}H_{43}N_3O_6$: C, 66.54; H, 7.94; N, 7.76. Found: C, 66.75; H, 8.09; N, 8.04%.

*Preparation of hydrazone **7***

Following the general procedure, the condensation of **1** with isoniazide (**3**) gave hydrazone **7** as a pale yellow solid in 79% yield (1.535 g), mp, 140–142 °C. IR (KBr): 3193, 3038, 2871, 1651, 1594, 1550, 1521, 1396, 1342, 1295, 1183, 1106, 969, 815, 753, 682 cm^{-1}. ^{1}H-NMR (60 MHz, $CDCl_3$): δ, 10.19 (s, 1H, –NH–), 8.50 (d, 2H, $J = 6.5$ Hz, Ar–H), 8.13 (s, 1H, –CH=N–), 7.55 (d, 2H, $J = 6.5$ Hz, Ar–H), 7.33 (d, 2H, $J = 7.5$ Hz, Ar–H), 6.45 (d, 2H, $J = 7.5$ Hz, Ar–H), 3.73–3.26 (m, 24H, > NCH_2CH_2O–). Anal. Calcd for $C_{25}H_{34}N_4O_6$: C, 61.73; H, 6.99; N, 11.52. Found: C, 61.87; H, 6.84; N, 11.24%.

*Preparation of hydrazone **9***

Following the general procedure, the condensation **1** with 4-nitrobenzoic hydrazide (**4**) gave the hydrazone **9** as a yellow solid in 83% yield (1.759 g), mp, 160–163 °C. IR (KBr): 3191, 3033, 2950, 2872, 1644, 1611, 1592, 1519, 1401, 1350, 1292, 1135, 1122, 1086, 818, 713, 664 cm^{-1}. ^{1}H-NMR (300 MHz, $CDCl_3$): δ, 11.08 (s, 1H, –NH–), 8.25 (s, 1H, –CH=N–), 8.17 (d, 2H, $J = 7.5$ Hz, Ar–H), 7.95 (d, 2H, $J = 7.5$ Hz, Ar–H), 7.49 (d, 2H, $J = 8.5$ Hz, Ar–H), 6.62 (d, 2H, $J = 8.5$ Hz, Ar–H), 3.78–3.31 (m, 24H, >NCH_2CH_2O–). Anal. Calcd for $C_{26}H_{34}N_4O_8$: C, 58.87; H, 6.42; N, 10.57. Found: C, 59.08; H, 6.16; N, 10.76%.

Synthesis of oxadiazoles **6**, **8** and **10**: general procedure

To a stirred solution of appropriate hydrazone (2 mmol) in dry acetone (50 mL) was added $KMnO_4$ (1.106 g, 7 mmol) portionwise during 1 h. The reaction mixture was continued to be stirred at room temperature for 4 h whereby the pink reaction turned brownish. The reaction mixture was then filtered through a pad of celite and the filtrate was concentrated to get a crude product solid. The crude was purified by SiO_2 column chromatography using $CHCl_3$:CH_3OH (99:1) as an eluent to obtain the desired oxadiazole products.

*Preparation of 2-(4-N-phenylaza-18-crown-6)-5-(4-t-butylphenyl)-1,3,4-oxadiazole (**6**)*

Following the general procedure, the oxidative cyclization of **5** gave oxadiazole **6** as a pale yellow oil in 52% yield (0.560 g). IR (KBr): 2880, 2869, 1610, 1503, 1397, 1351, 1271, 1193, 1115, 956, 843, 752, 710 cm^{-1}. ^{1}H-NMR (300 MHz, $CDCl_3$): δ, 8.03 (d, 2H, $J = 8.4$ Hz, Ar–H), 7.97 (d, 2H, $J = 6.9$ Hz, Ar–H), 7.53 (d, 2H, $J = 8.4$ Hz, Ar–H), 6.81 (d, 2H, $J = 6.9$ Hz, Ar–H), 3.72 (t, 4H, >NCH_2CH_2O–), 3.67–3.59 (m, 20H, –OCH_2CH_2–), 1.37 (s, 9H, Ar–$C(CH_3)_3$). Anal. Calcd for $C_{30}H_{41}N_3O_6$: C, 66.79; H, 7.61; N, 7.79. Found: C, 67.08; H, 7.70; N, 8.09%.

*Preparation of 2-(4-N-phenylaza-18-crown-6)-5-(4-pyridyl)-1,3,4-oxadiazole (**8**)*

Following the general procedure, the oxidative cyclization of **7** afforded oxadiazole **8** as a yellow solid in 54% yield (0.523 g), mp, 108–110 °C. IR (KBr): 2861, 1611, 1498, 1399, 1350, 1197, 1122, 987, 822, 740, 699 cm^{-1}. ^{1}H-NMR (300 MHz, $CDCl_3$): δ, 8.83 (d, 2H, $J = 6.5$ Hz, Ar–H), 8.03 (d, 2H, $J = 6.5$ Hz, Ar–H), 7.96 (d, 2H, $J = 8.7$ Hz, Ar–H), 6.82 (d, 2H, $J = 8.7$ Hz, Ar–H), 3.75 (t, 4H, >NCH_2CH_2O–), 3.67–3.59 (m, 20H, –OCH_2CH_2–). Anal. Calcd for $C_{25}H_{32}N_4O_6$: C, 61.98; H, 6.61; N, 11.57. Found: C, 62.21; H, 6.50; N, 11.73%.

*Preparation of 2-(4-N-phenylaza-18-crown-6)-5-(4-nitrophenyl)-1,3,4-oxadiazole (**10**)*

Following the general procedure, the oxidative cyclization of **9** afforded oxadiazole **10** as an orange solid in 51% yield (0.538 g), mp 142–145 °C. IR (KBr): 2866, 1613, 1519, 1499, 1402, 1349, 1296, 1197, 1118, 855, 739, 708 cm^{-1}. ^{1}H-NMR (300 MHz, $CDCl_3$): δ, 8.37 (d, 2H, $J = 8.5$ Hz, Ar–H), 8.25 (d, 2H, $J = 8.5$ Hz, Ar–H), 8.02 (d, 2H, $J = 8.9$ Hz, Ar–H), 6.72 (d, 2H, $J = 8.9$ Hz, Ar–H), 3.84 (t, 4H, >NCH_2CH_2O–), 3.72–3.65 (m, 20H, –OCH_2CH_2–). Anal. Calcd for $C_{26}H_{32}N_4O_8$: C, 59.09; H, 6.06; N, 10.61. Found: C, 58.80; H, 6.29; N, 10.74%.

Results and discussion

Spectrophotometric investigation of **6**, **8** and **10**

The absorption spectra of **6**, **8** and **10** measured in acetonitrile (ACN) showed two absorption bands; a higher energy band attributable to locally excited (LE) state appeared at λ_{max} at 257, 288 and 310 nm, respectively, whereas the absorption maxima due to intramolecular

charge transfer (ICT) excitations appeared at longer λ_{max} at 339, 350 and 386 nm, respectively. The ICT absorption bands were increasingly red shifted in the order **10** > **8** > **6** which is consistent with increasing acceptor character in going from *t*-butylphenyl to 4-pyridyl to 4-nitrophenyl substituents.

Since ICT bands in donor acceptor chromophores are sensitive to solvent polarity [16], we also examined the UV–Vis and fluorescence spectra of **6**, **8** and **10** in solvents of different polarities and the results are collected in Table 1. The fluorescence spectra were recorded by excitations at the absorption maxima observed in the respective solvents. The chromophore **10** is non-emissive on account of quenching by the $-NO_2$ group.

As can be seen from the Table 1, the ICT bands of **6**, **8** and **10** appeared slightly red shifted in solvents of lower polarities viz cyclohexane and chloroform compared to more polar ACN and MeOH. In cyclohexane the ICT bands of **6**, **8** and **10** appeared at 353, 370 and 397 nm, respectively while the absorption maxima in highly polar MeOH were blue shifted to 343, 357 and 382 nm, respectively. The increase in the blue shifts in changing the solvent from cyclohexane to MeOH follows the order **10** > **8** > **6** and implies that higher the ICT character, larger is the blue shifts. Clearly, chromophores **6**, **8** and **10** are subject to negative solvatochromism. The latter phenomenon has been encountered in certain dyes and dipolar molecules, [17, 18] and is believed to originate as a consequence of greater stabilization of the ground states relative to the excited states in solvents of increasing polarity [19].

However, the fluorescence spectra suffered significant red shifts in solvents of increasing polarity. When **6** and **8** (**10** being nonradiative) were excited at their respective absorption maxima, structureless ICT emission bands showing increasing red shifts in more polar solvents were observed. For the case of **6**, the emission band at 386 nm in cyclohexane was red shifted to 466 nm in MeOH, with a $\Delta\lambda_{em}$ of 81 nm. For chromophore **8**, with a higher degree of the ICT character than **6**, the emission band shifted from 398 nm in cyclohexane to 576 nm in methanol with a relatively massive $\Delta\lambda_{em}$ of 178 nm. As shown in Table 1, the solvent induced red shifts follow the order MeOH > ACN > $CHCl_3$ > cyclohexane. These finding are characteristic of the highly polar nature of the excited states. Higher Stokes shifts of **8** relative to **6** in all the solvents examined (see Table 1) also support polar nature of the excited states. It is proposed that with increasing solvent polarity, the excited states get progressively stabilized compared to the ground states. Consequently, the emissions then occur from highly relaxed Frank–Condon states, producing red shifted emissions in solvents of increasing polarity [20].

Table 1 UV–Vis and fluorescence data of **6**, **8** and **10** in various solvents

Solvent	**6**		**8**		**10**[a]
	λ_{abs} (nm)	λ_{em} (nm)	λ_{abs} (nm)	λ_{em} (nm)	λ_{abs} (nm)
Cyclohexane	353	385	370	398	397
Chloroform	341	402	358	482	395
Acetonitrile	339	443	350	524	386
Methanol	343	466	357	576	382

[a] Non-fluorescence system

UV–Vis spectral studies of **6**, **8** and **10** in the presence of metal ions

The UV–Vis profiles of **6**, **8** and **10** were investigated in ACN in the presence of biologically significant Li, Na, K, Mg, Ca and Ba ions as their perchlorate salts. The spectral changes are shown in Figs. 1–3 and the results are summarized in Table 2. Li^+, Na^+, K^+ and Mg^{2+} failed to elicit appreciable changes in the UV–Vis spectra, with the blue shifts of only 1–3 nm being detected in the ICT bands associated with the host molecules. Insignificant responses in the absorption spectra in the company of these cations imply rather weak ground state binding interactions with **6**, **8** and **10**.

However, UV–Vis spectra of **6**, **8** and **10** were significantly modified upon adding Ba^{2+} and Ca^{2+} perchlorates. Addition of Ca^{2+} to an ACN solutions of **6**, **8** and **10** induced blue shifts of the original ICT bands by 21, 20 and 29 nm, respectively. In comparison to Ca^{2+}, Ba^{2+} addition resulted in even larger blue shifts in the original ICT bands of **6**, **8** and **10** by 42, 58 and 65 nm, respectively. Such large blue shifts are characteristics of donor acceptor

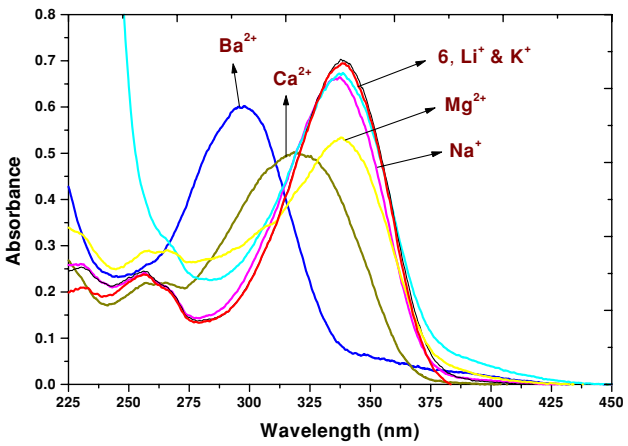

Fig. 1 Absorption spectra of **6** (2.27×10^{-5} M) in CH_3CN before and after addition of Ba^{2+} (6.81×10^{-5} M), Ca^{2+} (1.59×10^{-4} M), Mg^{2+} (3.41×10^{-4} M), Li^+ (4.31×10^{-4} M), Na^+ (4.54×10^{-4} M) and K^+ (4.09×10^{-4} M). Metal ion conc. refer to saturated concentrations

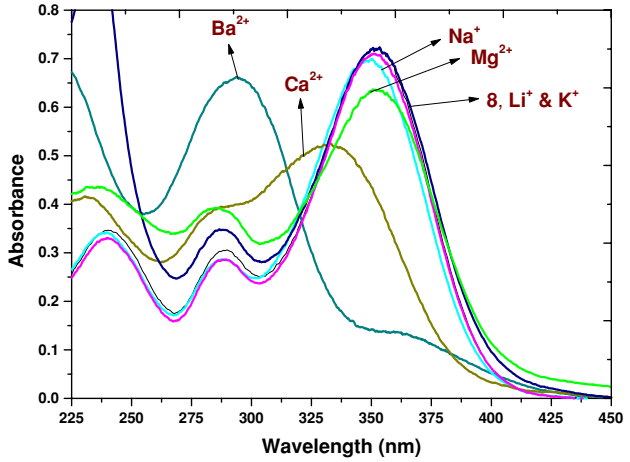

Fig. 2 Absorption spectra of **8** (2.27×10^{-5} M) in CH_3CN before and after addition of Ba^{2+} (1.36×10^{-4} M), Ca^{2+} (3.18×10^{-4} M), Mg^{2+} (4.54×10^{-4} M), Li^+ (4.99×10^{-4} M), Na^+ (4.31×10^{-4} M) and K^+ (5.67×10^{-4} M); metal ion conc. refer to saturated concentrations

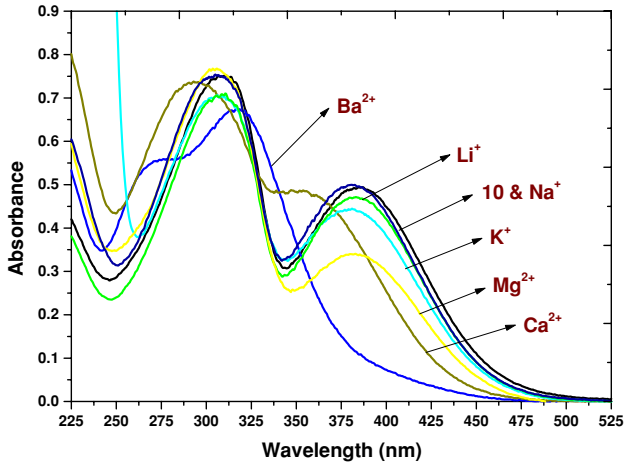

Fig. 3 Absorption spectra of **10** (2.27×10^{-5} M) in CH_3CN before and after addition of Ba^{2+} (2.27×10^{-4} M), Ca^{2+} (3.41×10^{-4} M), Mg^{2+} (5.45×10^{-4} M), Li^+ (5.90×10^{-4} M), Na^+ (4.77×10^{-4} M) and K^+ (6.13×10^{-4} M); metal ion conc. refer to saturated concentrations

systems in which metal ions coordination occurs at the donor sites [3, 10d]. The rationale for the blue shift is based on the consideration that metal ion complexation involving the aza-crown nitrogen will be stabilized the '*n*' orbitals relative to the π^*orbitals. Consequently, the energies of the $n\pi^*$ of the metal coordinated hosts would be raised relative to those of the free hosts, giving rise to the blue shifts. For the cases of **10**, which absorbs well into the visible region (λ_{max}, 386 nm), the original deep yellow solution turned colorless (λ_{max}, 320 nm) in the presence of Ba^{2+}. Thus, potential exists in **10** to function as a colorimetric sensor for Ba^{2+}.

For illustration, the spectrophotometric titration of **6** against incremental addition of Ba^{2+} is shown in Fig. 4. The original ICT band at 339 nm diminished in intensity as a new blue shifted band emerged at 297 nm. At a concentration of 6.81×10^{-5} mol, of Ba^{2+}, the 339 nm band is fully replaced by 297 nm band. A single well-defined isosbestic point is observed at 314 nm. This observation implies 1:1 binding stiochiometry which was also confirmed by the Job's plot [21] as shown in Fig. 5. For the cases of **8** and **10**, complete complexation occurred at Ba^{2+} concentrations of 13.62×10^{-5} and 22.7×10^{-5} mol and the corresponding isosbestic points were detected at 321 and 353 nm, respectively.

The stability constants, log K_S for the 1:1 complexation were determined from UV–Vis spectrophotometric data using non-linear curve fitting method [21] and the results are compiled in Table 3. The log K_S were found to follow the order **6** > **8** > **10** which reflects decreasing metal binding interactions of the aza-crown receptor in the series. This behavior is in accord with the decreased availability of the aza-crown nitrogen in metal binding interaction with the increase of the acceptor strengths of the aryl/heteroaryl substituents. For all the three chromoinophores, log K_S for Ba^{2+} were found to be markedly higher compared to coordinatively competing Ca^{2+} and Mg^{2+} and magnitude of log K_S followed the order $Ba^{2+} > Ca^{2+} \gg Mg^{2+} > Na^+ > Li^+ > K^+$.

Table 2 UV–Vis data of free and complexed ligands **6**, **8** and **10**

Complex	**6**			**8**			**10**		
	λ_{ICT} (nm)	$\Delta\lambda_{ICT}$ (nm)	ε_M (L mol^{-1} cm^{-1})	λ_{ICT} (nm)	$\Delta\lambda_{ICT}$ (nm)	ε_M (L mol^{-1} cm^{-1})	λ_{ICT} (nm)	$\Delta\lambda_{ICT}$ (nm)	ε_M (L mol^{-1} cm^{-1})
Neat	339	–	30,784	352	–	31,801	385	–	21,850
Ba^{2+}	297	42	26,449	294	58	29,092	320	65	29,691
Ca^{2+}	318	21	21,982	332	20	22,921	356	29	20,788
Mg^{2+}	338	1	23,493	351	1	28,035	382	3	14,929
Li^+	338	1	30,660	350	2	31,180	383	2	20,660
Na^+	336	3	29,071	349	3	30,701	380	5	21,380
K^+	338	1	29,427	351	1	31,629	381	4	19,511

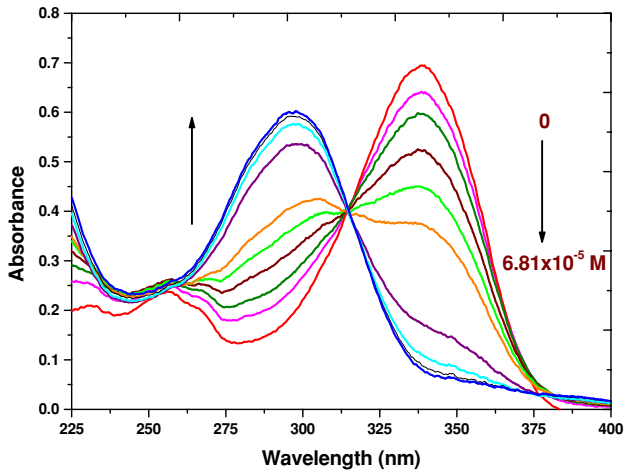

Fig. 4 Absorption spectra of **6** (2.27×10^{-5} M) in CH_3CN in the presence of increasing amount of $Ba(ClO_4)_2$ up to 6.81×10^{-5} M (saturation point)

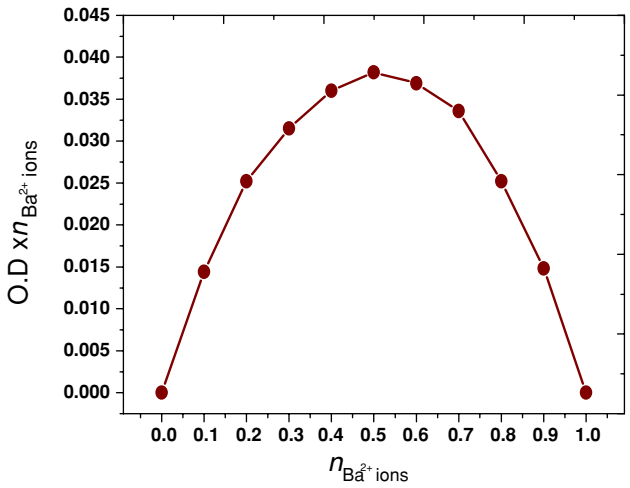

Fig. 5 Job's plot for the **6** + Ba^{2+} complex

In order to evaluate the selective binding of Ba^{2+}, we performed a competitive spectral analysis in the presence of a matrix of ions (Li^+, Na^+, K^+, Ca^{2+} and Mg^{2+} ions) (Fig. 6). Initially, a UV–Vis spectrum of **6** (2.27×10^{-5} M) in the presence of a matrix consisting of Ca^{2+} (1.59×10^{-4} M), Li^+, Na^+, K^+ and Mg^{2+} ions (each 4.54×10^{-4} M) was recorded. The resultant spectrum showed absorption maxima at 318 nm, which corresponds with the absorption spectrum of **6** obtained in the presence of Ca^{2+} alone (see Fig. 1). This result implies that Ca^{2+} interacts more strongly than Li^+, Na^+, K^+ and Mg^{2+}. Upon adding Ba^{2+} (6.81×10^{-5} M) to the above matrix, the 318 nm band was completely replaced by a new blue shifted absorption band at 297 nm. The latter band, which is reminiscent of the **6** + Ba^{2+} system is clearly due to the exclusive engagement of **6** with Ba^{2+} at the expense of other metal ions present in the matrix. This experiment manifests superior binding interaction of **6** with Ba^{2+} relative to Ca^{2+}, Mg^{2+}, Li^+, Na^+ and K^+. Similar behaviors were also noticed for **8** and **10**, which showed that in the matrix of ions, Ba^{2+} complexation occurs more selectively.

Fluorescence spectral studies of **6** and **8** in the presence of metal ions

As stated earlier, excitation of ACN solutions of **6** and **8** at their λ_{max} at 339 and 352 nm gave rise to structurless emission bands at 441 and 560 nm, respectively. The quantum yields (Φ_f) of **6** and **8** were calculated to be 0.737 and 0.302, respectively based on comparison with the integrated fluorescence spectra of the reference standard, coumarin 153 in cyclohexane ($\Phi_f = 0.90$) [22]. Lower Φ_f and higher Stokes shift for **8** (208 nm) than **6** (102 nm) are consistent with relatively higher ICT character of **8**, which turns this molecule largely non-radiative in nature [23].

Addition of Li^+, Na^+ and K^+ to **6** and **8** did not alter either the fluorescence intensity or fluorescence maxima, indicating the absence of any significant interaction with these metal ions. On the other hand, the emission maxims of **6** and **8** were markedly blue shifted in the company of Mg^{2+} ($\Delta\lambda_{em} = 6$ and 3 nm), Ca^{2+} ($\Delta\lambda_{em} = 13$ and 24 nm) and Ba^{2+} ($\Delta\lambda_{em} = 17$ and 30 nm). Consistent with the absorption spectra, the magnitude of emission blue shifts for both **6** and **8** were found to follow the order, $Ba^{2+} > Ca^{2+} \gg Mg^{2+} > Na^+ > Li^+ = K^+$. The photophysical data are collected in Table 4 (Figs. 7 and 8).

Table 3 Stability constants (log K_S) of metal complexes of **6**, **8** and **10**

Complex	Ionic diameter (Å)	log K_S[a] (**6** + M^{n+})	log K_S[a] (**8** + M^{n+})	log K_S[a] (**10** + M^{n+})
Neat	–	–	–	–
Ba^{2+}	2.68	3.96	3.72	2.75
Ca^{2+}	1.98	3.24	3.12	2.29
Mg^{2+}	1.32	2.43	2.20	1.60
Li^+	1.36	2.31	2.25	1.42
Na^+	1.94	2.36	2.29	1.64
K^+	2.66	1.65	1.45	1.51

[a] The stability constant was determined by non-linear fitting curve of absorption data [21]

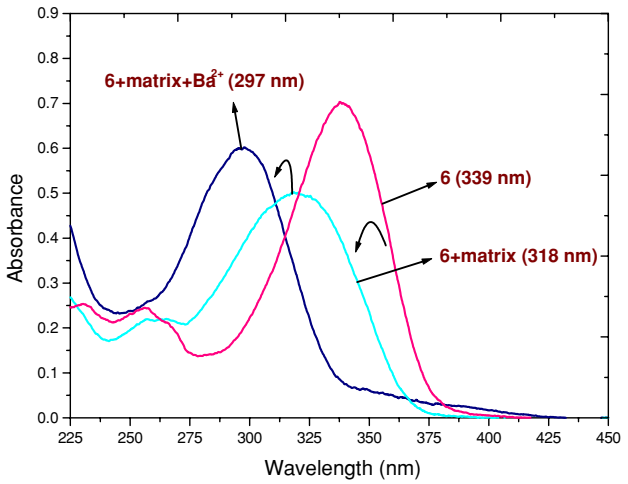

Fig. 6 Absorption spectra of **6** (2.27×10^{-5} M), **6** + Matrix [Ca^{2+} (1.59×10^{-4} M), Mg^{2+}, Li^{+}, Na^{+} and K^{+} (4.54×10^{-4} M), each] and **6** + Matrix + Ba^{2+} (6.81×10^{-5} M) in CH_3CN

Table 4 Fluorescence data of free and complexed ligands of **6** and **8**

Complex	**6**		**8**	
	λ_{em} (nm)	$\Delta\lambda_{em}$ (nm)	λ_{em} (nm)	$\Delta\lambda_{em}$ (nm)
Neat	441	–	560	–
Ba^{2+}	424	17	530	30
Ca^{2+}	428	13	536	24
Mg^{2+}	435	6	557	3
Li^{+}	440	1	559	1
Na^{+}	439	2	558	2
K^{+}	440	1	559	1

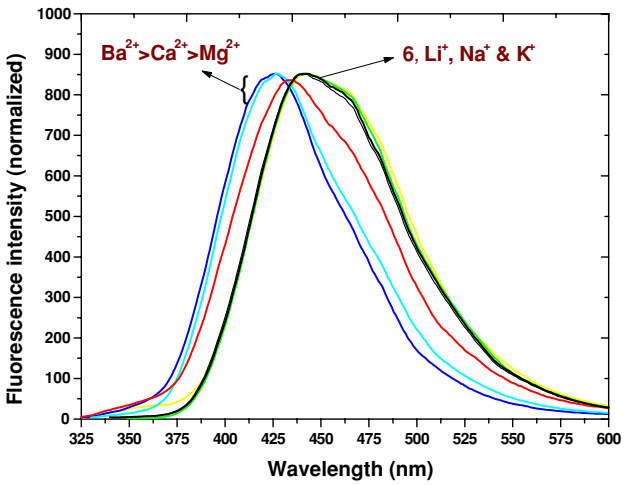

Fig. 7 Fluorescence spectra (corrected) of **6** (4.22×10^{-6} M) in CH_3CN before and after addition of Ba^{2+} (1.27×10^{-5} M), Ca^{2+} (2.95×10^{-5} M), Mg^{2+} (6.33×10^{-5} M), Li^{+} (8.01×10^{-5} M), Na^{+} (8.44×10^{-5} M) and K^{+} (7.59×10^{-5} M); excited at their respective isosbestic points

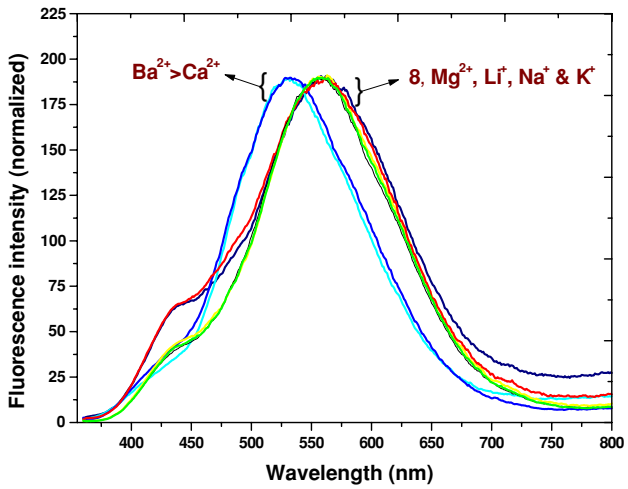

Fig. 8 Fluorescence spectra (corrected) of **8** (4.51×10^{-6} M) in CH_3CN before and after addition of Ba^{2+} (2.71×10^{-5} M), Ca^{2+} (6.31×10^{-5} M), Mg^{2+} (9.02×10^{-5} M), Li^{+} (9.92×10^{-5} M), Na^{+} (8.57×10^{-5} M) and K^{+} (1.13×10^{-4} M); excited at their respective isosbestic points

Discussion on the binding profile of **6**, **8** and **10**

The absorption spectra of chromoionophores **6**, **8** and **10** were solvent dependent, displaying a slight negative solvatochromism. However, fluorescence maxima experienced significant red shifts in response to increasing solvent polarity. The solvent induced red shifts followed the order MeOH > ACN > $CHCl_3$ > cyclohexane. These finding are characteristic of the polar nature of the excited states with the emission occurring from highly relaxed Frank–Condon states. *N*-Phenylaza-18-crown-6, carrying electron-withdrawing groups reportedly exhibit weak binding interactions with hard alkali metal ions [24]. Similar behavior has been observed with **6**, **8** and **10**, which incorporate aryl/pyridyloxadiazoles as the acceptor groups. Among the divalent metal ions investigated, Mg^{2+} exhibited insignificant photophysical perturbations with all the three chromoionophores. Higher charge density of 0.75 of Mg^{2+} (for Ba^{2+} and Ca^{2+}, the charge densities are 0.24 and 0.13, respectively) [10c] and its small ionic radii of 1.32 Å are presumably not compatible with the larger cavity size and softer nature of *N*-phenylaza-18-crown-6 receptor. The stronger binding of Ba^{2+} ion compared to Ca^{2+} is in accord with its ionic diameter of 2.68 Å, which is complimentary to 2.6–3.2 Å cavity size of the monoaza-18-crown-6 ether. Up on metal ion complexation, the aza-crown nitrogen is decoupled from conjugation, causing a decrease in the ICT character. Hence, the blue shifts in the absorption and emission maxima are entirely expected.

The metal ion binding interaction follows the order $Ba^{2+} > Ca^{2+} \gg Na^{+} > Li^{+} = K^{+} = Mg^{2+}$ and the log K_S, determined spectrophotometrically were larger for **6**

compared to **8** and **10**. This is understandable in view of the presence of an electron withdrawing pyridyl and nitrophenyl groups, which diminish the metal ion binding ability of the aza-crown ether in **8** and **10**. Available comparisons indicate that log K_S derived from our systems are comparable or better than those reported for some known *N*-phenylaza-18-crown-6 dyes [10d, 25]. It is noteworthy that the blue shifts in the λ_{ICT} of **6** and **8** in the presence of metal ions are substantially larger than observed in their fluorescence emission spectra. The reduced levels of blue shifts in the emission spectra imply relatively weaker cation—aza-crown interaction in the excited states compared to the ground states.

Conclusion

In conclusion, chemoionophores **6**, **8** and **10**, constitute potentially interesting Ba^{2+} sensitive probes due to their relatively high binding interaction for Ba^{2+} compared to the biologically interfering Ca^{2+} as well as Mg^{2+}. Though not fluorescent, chromophore **10** is of particular interest since, upon addition of Ba^{2+}, its deep yellow colored solution turned colorless, an event that can be visualized with naked eye.

Acknowledgement Thanks are due to the B.R.N.S., Government of India for the financial support.

References

1. (a) De Silva, A.P., Gunaratne, H.Q.N., Gunnlaugsson, T., Huxley, A.J.M., McCoy, C.P., Rademacher, J.T., Rice, T.E.: Signaling recognition events with fluorescent sensors and switches. Chem. Rev. **97**, 1515–1566 (1997); (b) Buhlmann, P., Pretsch, E., Bakker, E.: Carrier-based ion-selective electrodes and bulk optodes. 2. Ionophores for potentiometric and optical sensors. Chem. Rev. **98**, 1593–1687 (1998)
2. (a) Pedersen, C.J.: Cyclic polyethers and their complexes with metal salts. J. Am. Chem. Soc. **89**, 7017–7036 (1967); (b) Poonia, N.S., Bajaj, A.V.: Coordination chemistry of alkali and alkaline earth cations. Chem. Rev. **79**, 389–445 (1979); (c) Izatt, R.M., Bradshaw, J.S., Nielsen, S.A., Lamb, J.D., Christensen, J.J., Debabrata, S.: Thermodynamic and kinetic data for cation-macrocycle interaction. Chem. Rev. **85**, 271–339 (1985); (d) Gokel, G.W.: Crown Ethers and Cryptands. The Royal Society of Chemistry, Cambridge (1991)
3. (a) Lednev, I.K., Hester, R.E., Moore, J.N.: Benzothiazolium styryl dyes containing a monoazacrown ether: protonation and complexation with metal and ammonium cations in solution. J. Chem. Soc., Faraday Trans. **93**, 1551–1558 (1997); (b) Lednev, I.K., Hester, R.E., Moore, J.N.: A cation-specific, light-controlled transient chromoionophore based on a benzothiazolium styryl azacrown ether dye. J. Am. Chem. Soc. **119**, 3456–3461 (1997)
4. (a) Letard, J.F., Lapouyade, R., Rettig, W.: Synthesis and photophsical study of 4-(N-monoaza-15-crown-5) stilbenes forming PICT states and their complexation with cations. Pure Appl. Chem. **65**, 1705–1712 (1993); (b) Lewis, J.D., Moore, J.N.: Cation sensors containing a (bpy)$Re(CO)_3$ group linked to an azacrown ether via an alkenyl or alkynyl spacer: synthesis, characterisation, and complexation with metal cations in solution. J. Chem. Soc., Dalton Trans. 1376–1385 (2004) and references cited therein; (c) Yoshida, K., Mori, T., Wanatabe, S., Kawai, H., Nagamura, T.: Synthesis and metal ion-sensing properties of fluorescent PET chemosensors based on the 2-phenylimidazo[5,4-a]anthraquinone chromophore. J. Chem. Soc., Perkin Trans. **2**, 393–397 (1999)
5. (a) Ji, H.-F., Dabestani, R., Brown, G.M.: A supramolecular fluorescent probe, activated by protons to detect cesium and potassium ions, mimics the function of a logic gate. J. Am. Chem. Soc. **122**, 9306–9307 (2000); (b) Xue, G., Bradshaw, J.S., Dalley, N.K., Savage, P.B., Izatt, R.M., Prodi, L., Montalti, M., Zaccheroni, N.: The synthesis of azacrown ethers with quinoline-based sidearms as potential zinc(II) fluorophores. Tetrahedron **58**, 4809–4812 (2002); (c) He, H., Mortellaro, M.A., Leiner, A.J.P., Fraatz, R.J., Tusa, J.K.: A fluorescent sensor with high selectivity and sensitivity for potassium in water. J. Am. Chem. Soc. **125**, 1468–1469 (2003); (d) Pearson, A.J., Xiao, W.: Fluorescence and NMR binding studies of *N*-aryl-*N*′-(9-methylanthryl)diaza-18-crown-6 derivatives. J. Org. Chem. **68**, 5369–5376 (2003); (e) Mashraqui, S.H., Vashi, D., Sundaram,. S.: Synthesis, optical spectral studies of photoemmitive benzopyranone crown ether and its application for metal ion extraction. Indian J. Chem. **45B**, 1269–1273 (2006); (f) De Silva, A.P., Gunaratne, H.Q.N., Lynch, P.L.M., Maguire, G.E.M., McCoy, C.P., Sandanayake, K.R.A.S., Bissell, R.A.: Fluorescent PET (photoinduced electron transfer) sensors. Top. Curr. Chem. **168**, 243–264 (1993)
6. (a) Bourson, J., Pouget, J., Valeur, B.: Ion-responsive fluorescent compounds. 4. Effect of cation binding on the photophysical properties of a coumarin linked to monoaza- and diaza-crown ethers. J. Phys. Chem. **97**, 4552–4557 (1993); (b) Miteeva, N., Enchev, V., Antonov, L., Deligeorgiev, T., Mitewa, M.: Spectroscopic study on the complexation of an aza-15-crown-5 containing chromof1uoroionophore with Ba^{2+} and Ca^{2+} cations. J. Incl. Phenom., Mol. Recognit. Chem. **20**, 323–333 (1995); (c) Rurack, M., Kollmannsberger, U., Daub, R.-G.J.: A selective and sensitive fluoroionophore for Hg^{II}, Ag^{I}, and Cu^{II} with virtually decoupled fluorophore and receptor units. J. Am. Chem. Soc. **122**, 968–969 (2000); (d) Jiwan, J.L.H.: Photophysical and complexing properties of new fluoroionophores based on coumarin 343 linked to rigidified crown-ethers. J. Photochem. Photobiol. A.: Chem. **162**, 599–607 (2004); (e) Chen, T., Huang, W.-P.: A highly selective fluorescent chemosensor for lead ions. J. Am. Chem. Soc. **124**, 6246–6247 (2002); (f) Descalzo, A.B., Martinez-Manez, R., Radeglia, R., Rurack, K., Soto, J.: Coupling selectivity with sensitivity in an integrated chemosensor framework: design of a Hg^{2+}-responsive probe, operating above 500 nm. J. Am. Chem. Soc. **125**, 3418–3419 (2003); (g) Gunnlaugsson, T., Nieuwenhuyzen, M., Richard, L., Thoss, V.: A novel optically based chemosensor for the detection of blood Na^+. Tetrahedron Lett. **42**, 4725–4728 (2001); (h) Gunnlaugsson, T., Leonard, J.P.: Synthesis and evaluation of colorimetric chemosensors for monitoring sodium and potassium ions in the intracellular concentration range. J. Chem. Soc., Perkin Trans. **2**, 1980–1985 (2002); (i) Yang, Q.-Z., Wu, L.-Z., Zhang, H., Chen, B., Wu, Z.-X., Zhang, L.-P., Tung, C.-H.: A luminescent chemosensor with specific response for Mg^{2+}. Inorg. Chem. **43**, 5195–5197 (2004); (j) Liu, L.-H., Zhang, H., Li, A.-F., Xie, J.-W., Jiang, Y.-B.: Intramolecular charge transfer dual fluorescent sensors from 4-(dialkylamino)benzanilides with metal binding site within electron acceptor. Tetrahedron **62**, 10441–10449 (2006); (k) Mashraqui, S.H., Kumar, S., Vashi, D.: Synthesis, cation-binding and optical spectral studies of photoemmitive benzothiazole crown ethers. J. Incl. Phenom., Macrocycl. Chem.

48, 125–130 (2004); (l) Mashraqui, S.H., Dhaval, V., Sundaram, S., Khan, T.B.: Aza-crown ether tethered with benzothiazole: synthesis and optical spectral studies. Indian J. Chem. **45B**, 815–819 (2006); (m) Costero, A.M., Gil, S., Sanchis, J., Peransi, S., Sanz, V., Gareth Williams, J.A.: Conformationally regulated fluorescent sensors. Study of the selectivity in Zn^{2+} versus Cd^{2+} sensing. Tetrahedron **60**, 6327–6334 (2004); (n) Bren, V.A.: Fluorescent and photochromic chemosensors. Russ. Chem. Rev. **70**, 1017–1036 (2001); (o) Crochet, P., Malval, J.-P.: Ren′e Lapouyade: new fluoroionophores from aniline dimer derivatives: a variation of cation signaling mechanism with the number of amino groups. Chem. Commun. 289–290 (2000); (p) Lewis, J.D., Moore, J.N.: Cation sensors containing a (bpy)$Re(CO)_3$ group linked to an azacrown ether via an alkenyl or alkynyl spacer: synthesis, characterisation, and complexation with metal cations in solution. Dalton Trans. 1376–1385 (2004)

7. (a) London, R.E.: Methods for measurement of intracellular magnesium: NMR and fluorescence. Annu. Rev. Physiol. **53**, 241–258 (1991); (b) Murphy, E., Freudenrich, C.C., Lieberman, M.: Cellular magnesium and sodium/magnesium exchange in heart cells. Annu. Rev. Physiol. **53**, 273–287 (1991); (c) Jung, D.W., Chapman, C.J., Baysal, K., Pfeiffer, D.R., Brierley, G.P.: On the use of fluorescent probes to estimate free Mg^{2+} in the matrix of heart mitochondria. Arch. Biochem. Biophys. **332**, 19–29 (1996); (d) Hurley, T.W., Ryan, M.P., Brinck, R.W.: Changes of cytosolic Ca^{2+} interfere with measurements of cytosolic Mg^{2+} using mag-fura-2. Am. J. Physiol. Cell Physiol. **263**, 300–307 (1992); (e) Watanable, S., Ikishima, S., Matsuo, T., Yoshida, K.: A luminescent metalloreceptor exhibiting remarkably high selectivity for Mg^{2+} over Ca^{2+}. J. Am. Chem. Soc. **123**, 8402–8403 (2001); (f) Suzuki, Y., Saito, N., Komatsu, H., Citterio, D., Kubota, T., Kitamura, Y., Oka, K., Suzuki, K.: Design and application of novel fluorescent indiacators for Mg^{2+}. Anal. Sci. Suppl. **17**, i1451–i1454 (2001); (g) Yang, Q.-Z., Wu, L.-Z., Zhang, H., Wu, Z.-X., Zhang, L.-P., Tung, C.-H.: A luminescent chemosensor with specific response for Mg^{2+}. Inorg. Chem. **43**, 5195–5197 (2004); (h) Pearson, A.J., Xiao, W.: Fluorescence and NMR binding studies of *N*-aryl-*N*′-(9-methylanthryl)diaza-18-crown-6 derivatives. J. Org. Chem. **68**, 5369–5376 (2003); (i) Morozumi, T., Anada, T., Nakamura, H.: New fluorescent "off-on" behavior of 9-anthryl aromatic amides through controlling the twisted intramolecular charge transfer relaxation process by complexation with metal ions. J. Phys. Chem. B. **105**, 2923–2931 (2001)
8. Yu, S.-B., Watson, A.D.: A review on the subject of medical X-ray examinations and metal based contrast agents. Chem. Rev. **99**, 2353–2378 (1999)
9. Cook, A.G., Weinstein, P., Centeno, J.A.: Health effects of natural dust: role of trace elements and compounds. Biol. Trace Elem. Res. **103**, 1–15 (2005)
10. (a) Mashraqui, S.H., Sundaram, S., Khan, T.: Benzimidazole-chalcone: a selective intramolecular charge-transfer probe for biologically important zinc ions. Chem. Lett. **35**, 786–787 (2006); (b) Mashraqui, S.H., Khan, T., Sundaram, S., Betkar, R., Chandiramani, M.: A new intramolecular charge transfer receptor as a selective ratiometric 'off-on' sensor for Zn^{2+}. Tetrahedron Lett. **48**, 8487–8490 (2007); (c) Mashraqui, S.H., Sundaram, S., Bhasikuttan, A.C., Kapoor, S., Sapre, A.V.: Novel fluoroionophores incorporating diaryl-1,3,4-oxadiazole and aza-crown ring. Potentially sensitive Mg^{2+} ion sensor. Sensors Actuators B **122**, 347–350 (2007); (d) Mashraqui, S.H., Sundaram, S., Bhasikuttan, A.C.: New ICT probes: synthesis and photophysical studies of N-phenylaza-15-crown-5 aryl/heteroaryl oxadiazoles under acidic condition and in the presence of selected metal ions. Tetrahedron **63**, 1680–1688 (2007)
11. Dix, J.P., Vögtle, F.: Ligand structure and complexation L. Ion-selective crown ether dyes. Chem. Ber. **113**, 457–470 (1980)
12. Lee, D.W., Kwon, K.-Y., Jung, J., Park, Y., Kim, Y.-R., Hwang, I.-W.: Luminescence properties of structurally modified PPVs: PPV derivatives bearing 2-(4-*tert*-butylphenyl)-5-phenyl-1,3,4-oxadiazole pendants. Chem. Mater. **13**, 565–574 (2001)
13. Oruc, E.E., Rollas, S., Kandemirli, F., Shvets, N., Dimoglo, A.S.: 1,3,4-Thiadiazole derivatives, synthesis, structure elucidation, and structure-antituberculosis activity relationship investigation. J. Med. Chem. **47**, 6760–6767 (2004)
14. Reddy, P.S.N., Reddy, P.: Fusion of aroylhydrazines with acids—a new synthesis of 2,5-diaryl-1,3,4-oxadiazoles. Indian J. Chem., Sect. B **26**, 890–891 (1987)
15. Bartsch, R.A., Yang, I.W., Jeon, E.G., Walkowiak, W., Charewicz, W.A.: Selective transport of alkali metal cations in solvent extraction by proton-ionizable dibenzocrown ethers. J. Coord. Chem. **27**, 75–85 (1992)
16. Chattopadhyay, N., Serpa, C., Pereira, M.M., De Melo, J.S., Arnaut, L.G., Formosinho, S.J.: Intramolecular charge transfer of *p*-(dimethylamino) benzethyne: a case of nonfluorescent ICT state. J. Phys. Chem. A **105**, 10025–10030 (2001)
17. (a) Rurack, K., Dekhtyar, M.L., Bricks, J.L., Resch-Genger, U., Rettig, W.: Quantum yield switching of fluorescence by selectively bridging single and double bonds in chalcones: involvement of two different types of conical intersections. J. Phys. Chem. A. **103**, 9626–9635 (1999)
18. (a) Rurack, K., Bricks, J.L., Reck, G., Radeglia, R., Resch-Genger, U.: Chalcone-analogue dyes emitting in the near-infrared (NIR): influence of donor-acceptor substitution and cation complexation on their spectroscopic properties and X-ray structure. J. Phys. Chem. A. **104**, 3087–3109 (2000); (b) Kosower, E.M.: Intramolecular donor-acceptor systems. 9. Photophysics of (phenylamino)naphthalenesulfonates: a paradigm for excited-state intramolecular charge transfer. Acc. Chem. Res. **15**, 259–266 (1982)
19. (a) Kim, K., Funabiki, H., Muramatsu, K., Shibata, S.H., Kim, H., Shiozaki, H., Matsui, H.M.: Negative solvatochromism of azo dyes derived from (dialkylamino)thiazole dimers. Chem. Commun. 753–754 (2000); (b) Allen, D.W., Li, X.: Solvatochromic and halochromic properties of some phosphonioarylimino- and phosphonioarylazo-phenolate betaine dyes. J. Chem. Soc., Perkin Trans **2**, 1099–1104 (1997)
20. (a) Kamlet, M.J., Abboud, J.L., Taft, R.W.: The solvatochromic comparison method. 6. The π^* scale of solvent polarities. J. Am. Chem. Soc. **99**, 6027–6038 (1977); (b) Reichardt, C.: Solvatochromic dyes as solvent polarity indicators. Chem. Rev. **94**, 2319–2358 (1994); (c) Herbich, J., Kapturkiewicz, A., Nowacki, J., Golinski, J., Dabrowski, Z.: Intramolecular excited charge-transfer states in donor-acceptor derivatives of naphthalene and azanaphthalenes. Phys. Chem. Chem. Phys. **3**, 2438–2449 (2001); (d) Braun, D., Rettig, W., Delmond, S., Letard, J.-F., Lapouyade, R.: Amide derivatives of DMABN: a new class of dual fluorescent compounds. J. Phys. Chem. A **101**, 6836–6841 (1997)
21. Mohanty, J., Bhasikuttan, A.C., Nau, W.M., Pal, H.: Host-guest complexation of neutral red with macrocyclic host molecules: contrasting pK_a shifts and binding affinities for cucurbit[7]uril and -cyclodextrin. J. Phys. Chem. B **110**, 5132–5138 (2006)
22. Jones II, G., Jackson, W.R., Choi, C.-Y., Bergmark, W.R.: Solvent effects on emission yield and lifetime for coumarin laser dyes. Requirements for a rotatory decay mechanism. J. Phys. Chem. **89**, 294–300 (1985)
23. Rurack, K., Dekhtyar, M.L., Bricks, J.L., Resch-Genger, U., Rettig, W.: Quantum yield switching of fluorescence by selectively bridging single and double bonds in chalcones: involvement of two different types of conical intersections. J. Phys. Chem. A **103**, 9626–9635 (1999)
24. (a) Boila-Gockel, A., Junek, H.: Spacer-chromoionophores. Polymethine dye substituted azacrown ethers with increased

complexation ability. J. Prakt. Chem. **341**, 20–28 (1999); (b) Boila-Gockel, A., Fabian, W.M.F., Junek, H.: Syntheses with nitriles. Part 97. Synthesis and characterization of (aminocyanomethylene)indandione and -pyrazolone chromoionophores as extractants for alkali metal ions. Liebigs Ann. 397–402 (1996)

25. Lednev, I.K., Hester, R.E., Moore, J.N.: Benzothiazolium styryl dyes containing a monoazacrown ether: protonation and complexation with metal and ammonium cations in solution. J. Chem. Soc., Faraday Trans. **93**, 1551–1558 (1997)